Free Radical Biology and Medicine 55 (2013) 46–53

Contents lists available at SciVerse ScienceDirect

Free Radical Biology and Medicine

journal homepage: www.elsevier.com/locate/freeradbiomed

Original Contribution

Bicarbonate modulates oxidative and functional damage in ischemia–reperfusion

Bruno B. Queliconi [a], Thire B.M. Marazzi [a], Sandra M. Vaz [a], Paul S. Brookes [b], Keith Nehrke [b], Ohara Augusto [a], Alicia J. Kowaltowski [a,*]

[a] Departamento de Bioquímica, Instituto de Química, Universidade de São Paulo, 05508–900 São Paulo, SP, Brazil
[b] University of Rochester Medical Center, Rochester, NY 14642, USA

ARTICLE INFO

Article history:
Received 25 May 2012
Received in revised form
1 November 2012
Accepted 13 November 2012
Available online 27 November 2012

Keywords:
Carbonate radical
Ischemic damage
Heart
Caenorhabditis elegans
Free radicals

ABSTRACT

The carbon dioxide/bicarbonate (CO_2/HCO_3^-) pair is the main biological pH buffer. However, its influence on biological processes, and in particular redox processes, is still poorly explored. Here we study the effect of CO_2/HCO_3^- on ischemic injury in three distinct models (cardiac HL-1 cells, perfused rat heart, and *Caenorhabditis elegans*). We found that, although various concentrations of CO_2/HCO_3^- do not affect function under basal conditions, ischemia–reperfusion or similar insults in the presence of higher CO_2/HCO_3^- resulted in greater functional loss associated with higher oxidative damage in all models. Because the effect of CO_2/HCO_3^- was observed in all models tested, we believe this buffer is an important determinant of oxidative damage after ischemia–reperfusion.

Introduction

CO_2, formed in a multitude of intracellular reactions, is hydrated in a reaction catalyzed by carbonic anhydrase to carbonic acid (H_2CO_3), which deprotonates, generating bicarbonate (HCO_3^-). The CO_2/HCO_3^- pair, with a pK_a of 6.4, is the main physiological buffer, due mostly to its high concentration in biological compartments (extracellular fluid pH is ~7.2 [10,14]).

Interestingly, despite its ubiquity and abundance, biological activities of the CO_2/HCO_3^- pair have received very little attention, probably because there is little ability to control concentrations in vivo. Bicarbonate buffer, which is composed of ~1.3 mM CO_2 in equilibrium with 25 mM HCO_3^- in serum and 14 mM HCO_3^- intracellularly, has well-demonstrated redox effects (see [23] for a review). The first suggestion in this sense came from Hodgson and Fridovich in 1976 [15], who reported that xanthine oxidase-catalyzed luminescence was dependent on the presence of carbonate. After that, a series of studies demonstrated that the presence of CO_2/HCO_3^- stimulates the oxidation, peroxidation, and nitration of various biomolecules [2,3,21,24,27,34,42,43]. The mechanism through which CO_2/HCO_3^- stimulates these oxidations has been elucidated for peroxynitrite-mediated processes but remains uncovered in most cases because of methodological difficulties involving the detection of highly reactive intermediates, such as the carbonate radical (see [23] for a review).

Most studies addressing the role of CO_2/HCO_3^- in biological oxidations have been exclusively conducted in in vitro or, less commonly, in vivo systems to which oxidants were added exogenously, promoting overt oxidative stress followed by an evaluation of the effects of HCO_3^- [10]. This still leaves open the question if CO_2/HCO_3^- levels are relevant for oxidative injury resulting from reactive oxygen species (ROS)[1] generated endogenously in vivo under physiological or pathological conditions. The question is highly relevant because, owing to their reactive and diverse nature, ROS effects mostly result from localized intracellular reactions [6,39]. In addition, quantities of added oxidants may differ very significantly from those produced intracellularly, even under pathological conditions. The demonstration that CO_2/HCO_3^- levels affect tissues under physiologically relevant conditions would provide evidence, albeit indirect, of the participation of carbonate radicals in biologically relevant processes [23].

To address this point, we chose to study the effects of CO_2/HCO_3^- in ischemia–reperfusion (IR). IR occurs in important pathological conditions such as heart attack and stroke and involves a burst in ROS production and oxidative damage, mainly during

Abbreviations: DNPH, 2,4-dinitrophenylhydrazine; BCECF, 2′,7′-bis(carboxyethyl)-5(6)-carboxyfluorescein; BPM, beats per minute; DTT, dithiothreitol; IR, ischemia–reperfusion; AS, anoxia–starvation; NGM, normal growth medium; PLML, posterior lateral microtubule cell left; PLMR, posterior lateral microtubule cell right; ROS, reactive oxygen species; SDS, sodium dodecyl sulfate

* Corresponding author. Fax: +55 11 38155579.
E-mail address: alicia@iq.usp.br (A.J. Kowaltowski).

0891-5849/$ - see front matter © 2012 Elsevier Inc. All rights reserved.
http://dx.doi.org/10.1016/j.freeradbiomed.2012.11.007

reperfusion, that is a determinant of the final outcome of tissue damage [12,22,35]. Furthermore, because of the nature of these pathologies, which involve changes in local tensions of diluted gasses and modifications from oxidative to fermentative metabolism, CO_2/HCO_3^- levels are expected to change during IR and may, thus, have an important role in determining the extent of postischemic lesions.

The effects of CO_2/HCO_3^- levels on functional and oxidative damage after IR were tested in three distinct models, under conditions in which external pH was clamped despite the changes in CO_2/HCO_3^- concentrations. Our results show that CO_2/HCO_3^- levels contribute strongly toward postischemic functional loss and oxidative damage.

Materials and methods

Materials

All chemicals were of the highest purity available from Sigma (St. Louis, MO, USA), unless otherwise specified. BCECF was purchased from Molecular Probes (Eugene, OR, USA). Antibody sources are provided under Western blots.

Isolated heart perfusion

Heart perfusion was conducted as described previously [12]. Briefly, hearts were rapidly removed from male Sprague–Dawley rats (~300 g, 2–3 months of age) and Langendorff-perfused with oxygenated Krebs–Henseleit buffer (described below). Hearts were eliminated from the study if the time between rat death and the beginning of perfusion was longer than 3 min. All studies were conducted in accordance with guidelines for animal care and use established by the *Colégio Brasileiro de Experimentação Animal* and approved by the local animal ethics committee.

After isolation, the hearts were stabilized for 50 min and then subjected to 30 min ischemia and 60 min reperfusion. The reperfusion was conducted with buffers containing 0, 5, and 10% CO_2. The buffer for 0% CO_2 contained (in mmol/L) 118 NaCl, 1.2 KH_2PO_4, 4.7 KCl, 1.2 $MgSO_4$, 1.25 $CaCl_2$, 10 glucose, and 20 Na^+-Hepes, pH 7.4, gassed with pure O_2, at 37°C; that for 5% (in mmol/L) 118 NaCl, 17 $NaHCO_3$, 1.2 KH_2PO_4, 4.7 KCl, 1.2 $MgSO_4$, 1.25 $CaCl_2$, 10 glucose, and 20 Na^+-Hepes, pH 7.4, at 37 °C gassed with 95% O_2 + 5% CO_2; and that for 10% (in mmol/L) 118 NaCl, 25 $NaHCO_3$, 1.2 KH_2PO_4, 4.7 KCl, 1.2 $MgSO_4$, 1.25 $CaCl_2$, 10 glucose, and 20 Na^+-Hepes, pH 7.4, at 37 °C gassed with 90% O_2 + 10% CO_2. L-NAME (200 μM), when present, was added 10 min before ischemia and remained in the perfusate until the end of the reperfusion time.

Hemodynamic data were obtained using an electrode connected to a Powerlab Langendorff apparatus from ADInstruments. The pressure transducer was connected to a latex balloon and placed inside the left ventricle, as described previously [12].

Infarcted area

Quantification of the infarcted area was conducted as previously described [5,13]. Briefly, after reperfusion the heart was sliced and incubated in 1% triphenyltetrazolium chloride for 15 min. The infarcted area was quantified using ImageJ and is presented as a percentage of the total area of the slice. Each heart was sliced in three places and the areas from both sides were quantified by an unblinded scorer and averaged.

Cardiac HL-1 cell cultures and simulated cellular IR

Cardiac HL-1 cells were kindly donated by Professor William C. Claycomb. These cells maintain their cardiac phenotype during extended passages and present ordered myofibrils, cardiac-specific junctions, and voltage-dependent currents that are characteristic of a cardiac myocyte phenotype [7]. For routine growth, HL-1 cells were maintained in T-75 flasks at 37 °C in an atmosphere of 5% CO_2 in Claycomb medium (Sigma) supplemented with 0.1 mM norepinephrine, 100 U/ml penicillin, 100 U/ml streptomycin, 2 mM glutamine, and 10% fetal bovine serum. Experiments were conducted at 100% confluence, after trypsinization and resuspension in a standard buffer (pH 7.4) containing (in mmol/L) 137 NaCl, 20 Na-Hepes, 22 glucose, 5 Na-pyruvate, 20 taurine, 5 creatine, 5.4 KCl, 1 $MgCl_2$, and 1 $CaCl_2$.

Cell IR was simulated as previously described [11,12]. Briefly, 10^6 cells/ml were subjected to simulated ischemia by metabolic inhibition using 50 mM KCN and 2 mM 2-deoxyglucose added to standard cell buffer devoid of glucose and pyruvate for 90 min, followed by 5 min centrifugation and resuspension of the cell pellet in experiment buffer for simulated reperfusion. Control HL-1 cardiomyocytes were incubated with standard buffer solution during the entire experimental period and subjected only to centrifugations and washes. The standard buffer was gassed with 100% O_2 for the 0% CO_2 condition, and 25 mM $NaHCO_3$ was added to a buffer gassed with a mixture of 90% O_2 + 10% CO_2 for 10% CO_2 condition.

Cell viability

Cell viability was assessed by relative fluorescence of 50 μM ethidium bromide (Sigma–Aldrich) using a Hitachi F4500 spectrofluorimeter at excitation and emission wavelengths of 365 and 580 nm, respectively [11,12,17]. Cells were permeabilized with 0.1% Triton at the end of the each experiment to promote 100% cell death. The autofluorescence of ethidium bromide was subtracted from total fluorescence in the presence of cells, ethidium bromide, and Triton. Data are expressed as the percentage of total cells.

Intracellular pH measurements

pH measurements were conducted using the highly sensitive intracellular probe BCECF, with a modification of a described method [16,30]. Cells were trypsinized, washed, and resuspended in experimental buffer (described in the cell IR protocol) twice. Cells (10^6/ml) were incubated with 5 μM BCECF for 90 min, pelleted, and resuspended in experimental buffer. The readings were conducted using a Hitachi F4500 spectrofluorimeter with fixed emission at 535 nm. The excitation was scanned from 400 to 550 nm. After the measurement of the baseline fluorescence, calibration was conducted adding 10 mg/ml nigericin to allow from proton exchange across the plasma membrane and adding NaOH and HCl to promote maximal alkalization and acidification. The intracellular pH was calculated as described by the maker. Briefly, the formula used was $[H^+] = K_a((R - R_A)/(R_B - R))(F_{A(\lambda 2)}/F_{B(\lambda 2)})$, where R is the $F_{(\lambda 1)}/F_{(\lambda 2)}$ ratio of fluorescence intensities (F) measured at two wavelengths, λ1, 490 nm, and λ2, 440 nm, and the subscripts A and B represent the limiting values at the acidic and basic endpoints of the titration, respectively.

Caenorhabditis elegans culture and strains

C. elegans were cultured using standard techniques at 20 °C on normal growth medium (NGM) agar plates [4]. Synchronized young adults were used in the experiments. The strains used were Bristol N2 (wild type) and KWN85 (*him-5*(*e1490*)V, uIs22 (P*mec-18*::GFP)V).

C. elegans anoxia–starvation (AS)

IR in *C. elegans* was simulated by promoting AS followed by reoxygenation and feeding, as previously described [32,40,41].

C. elegans young adults were collected from NGM plates, washed three times, and resuspended in M9 medium (22 mM KH_2PO_4, 42 mM Na_2HPO_4, 86 mM NaCl, 1 mM $MgSO_4$, pH 7.0) supplemented with 20 mM Hepes. The animals were incubated in 100 µl of M9 in an open Eppendorf tube at 26 °C for 20 h under either 100 or 90% N_2 and 10% CO_2. After AS, *C. elegans* were moved to a seeded plate with a minimal amount of M9 and left to recover for another 24 h and then scored by an unblinded observer for viability and sensitivity to touch.

C. elegans neuron imaging

Animals were transferred to a 2% M9 agarose pad containing 0.1% tetramisole and 0.1% tricaine (EMS, Hatfield, PA, USA) and were imaged within 20 min of being placed under a coverslip. A Nikon Eclipse TE2000-U microscope (Nikon USA, Melville, NY, USA), Polychrome V monochromator (TILL Photonics, Gräfelfing, Germany), and Cooke Sensicam CCD (PCO-TECH, Romulus, MI, USA) were coordinated using TILLvisION software to obtain fluorescence images (470 nm excitation/535 nm emission) under a 100× oil objective.

Western blots

Western blots used 12% denaturing gels. Gels were transferred (4 h, 400 mV) onto polyvinylidene difluoride membranes. Protein was quantified by the Bradford technique. For carbonylation detection, 5 µg of protein was used per lane. Detection of 3-nitrotyrosine and methionine sulfoxide residues used 10 µg of protein.

The samples from hearts and cells were prepared by homogenizing the tissue or the cells in the presence of a RIPA buffer (135 mM NaCl, 50 mM Tris–HCl, 1% Nonidet P-40, 0.5% sodium deoxycholate, 0.1% SDS, and 1:10 Sigma proteinase inhibitor cocktail, pH 8) and frozen at −80 °C until use. For *C. elegans* samples, the live worms were selected after reperfusion and resuspended in buffer previously described in [5] (0.2 M Tris–HCl, 100 mM DTT, 20% glycerol, 10% SDS, and 1:10 Sigma proteinase inhibitor cocktail, pH 8), subjected to three freeze/thaw cycles (liquid nitrogen/boiling water), and frozen at −80 °C until use.

For the carbonylation Western blots, samples were treated as described before [8,26], or the OxyBlot kit from Millipore was used and the reactions were done as described by the manufacturer. Briefly, we added SDS to the samples to reach a final concentration of 12% and then subjected the proteins to a reaction with 2,4-dinitrophenylhydrazine (DNPH) for 30 min followed by the addition of a neutralization buffer. For detection, we used 1:5000 anti-DNP antibody from Sigma and 1:7000 anti-rabbit from Calbiochem. For other Western blots, we added the protein with sample buffer (20 µg). Antibody concentrations were anti-nitrotyrosine from Upstate, 1:5000; anti-mouse from Calbiochem, 1:5000; anti-methionine sulfoxide from Upstate, 1:5000; and anti-rabbit from Calbiochem and anti-phospho-Akt(Ser473) from Cell Signaling, 1:5000.

The blots were scanned and analyzed using ImageJ. Images were converted to 8 bits color and intensities of the whole lane were included. Blots were compared to the 0% CO_2 control or to the 0% CO_2 ischemic group. In the 3-nitrotyrosine blot, we ran a standard amount of nitrated protein to quantify modified tyrosine.

Statistics

All experiments presented were replicated at least three times, and statistical analysis was conducted using GraphPad Prism 5. Fig. 2A, B, D, and E were analyzed using two-way ANOVA followed by Bonferroni correction, and all other data were analyzed using Student *t* tests. Correlations were analyzed using linear fits. Differences were considered significant if $p < 0.05$.

Results

Our aim in this work was to evaluate the impact of CO_2/HCO_3^- on oxidative and functional tissue damage under the pathologically relevant condition of IR. Because CO_2/HCO_3^- is a vital buffer, and we wished to focus on the effects of CO_2/HCO_3^- itself, and not changes in pH, all extracellular solutions used in this study were buffered using Hepes, and the pH was carefully adjusted after gassing. Additionally, we questioned if, despite the clamped pH, changes in extracellular CO_2/HCO_3^- concentrations could result in alterations in intracellular pH. To address this question, we used cardiac HL-1 cells, a cell line that maintains the cardiac phenotype and has been extensively used to study cardiac IR (Fig. 1) [7,12,38]. Cells were loaded with the intracellular pH probe BCECF, and intracellular pH was measured in the absence or presence of CO_2/HCO_3^- (indicated as the percentage of gassed CO_2, 0 or 10%). We found that intracellular pH was indistinguishable under both incubation conditions (Fig. 1A). Thus, the conditions established allow for the evaluation of the biological role of CO_2/HCO_3^- independent of changes in physiological intracellular pH.

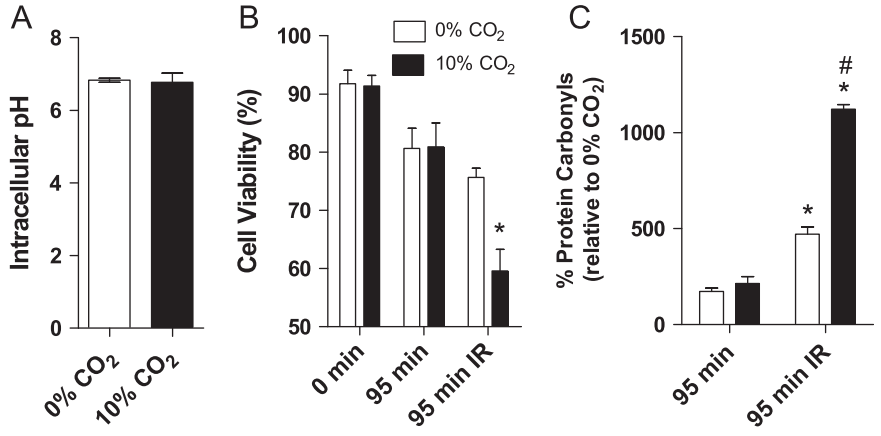

Fig. 1. Cardiac HL-1 cells present increased oxidative damage and loss of viability when subjected to IR in the presence of CO_2. (A) Intracellular pH was measured as described under Materials and methods, in the presence or absence of CO_2, after 95 min stabilization. (B) Cell viability was measured in the absence (open bars) or presence (filled bars) of 10% H_2CO_3/HCO_3^-. Cell viability was measured as described under Materials and methods, at 0 and 95 min, in the absence or presence of IR, as indicated and (C) Protein carbonyl levels were detected as described under Materials and methods and are shown as percentage of 0% CO_2 levels at 0 min. $^*p < 0.05$ relative to nonischemic, 95 min; $^{\#}p < 0.05$ relative to 95 min IR in 0% CO_2.

We then subjected the cells to simulated IR (see Materials and methods) in the presence of 0 and 10% CO_2 (Fig. 1B). We found that after IR, cells incubated in buffer containing CO_2/HCO_3^- (filled bars, 95 min IR) had significantly lower viability compared to cells incubated in the absence of CO_2/HCO_3^- (open bars). Indeed, cell viability in the absence of CO_2 was similar to that of cells subjected to 95 min incubation and centrifugations, but not IR. Cell viability before the ischemic intervention (0 min) and under nonischemic conditions (95 min) was similar in both CO_2/HCO_3^--containing and 0% CO_2 groups, indicating that changes in CO_2/HCO_3^- levels do not affect cell viability under physiological conditions, but exacerbate cell death after IR.

To verify if the loss of cell survival was associated with oxidative damage, we measured protein carbonyls in cell lysates. We found that incubation and centrifugation of samples for 95 min in the absence of IR increased carbonyl levels slightly relative to baseline in both 0 and 10% CO_2 (Fig. 1C, 95 min). However, after 95 min IR, very significant increments in protein carbonyl levels were observed, and this increase was substantially larger in 10% CO_2 samples. Together, these results demonstrate that the presence of CO_2/HCO_3^- substantially affects cell survival and oxidative damage after IR in cardiac cells.

Given the striking results of changes in CO_2/HCO_3^- concentrations in cells subjected to IR, we sought next to evaluate the effects of these on ischemic hearts. Langendorff-perfused rat hearts were either maintained for 150 min without any intervention (nonischemic) or subjected to IR as described under Materials and methods (Fig. 2). We found that the various gassed CO_2 concentrations (0, 5, or 10%) did not affect nonischemic heart beat rates (BPM; Fig. 2A) or left-ventricular developed pressure (Fig. 2B), a measure of cardiac function. Furthermore, the various CO_2 concentrations did not affect activating Akt phosphorylation, a known determinant of infarct injury (results not shown). On the other hand, ischemic hearts perfused with 10% CO_2 presented severely decreased BPM (Fig. 2D) and change in developed pressure (Fig. 2E) during reperfusion; the difference was significant both comparing the curves point by point (as shown in the figures) and integrating the area under the curve at reperfusion ($p < 0.05$ comparing 0 and 10% CO_2 using a t test, for both BPM and developed pressure). Indeed, 10% CO_2 hearts displayed an infarcted area that was double that observed in 0% CO_2 IR hearts (Fig. 2F). Overall, these results confirm, in a whole-heart model, that CO_2/HCO_3^- levels are a determinant of functional cardiac recovery after IR.

To evaluate if the changes in cardiac function observed were associated with oxidative damage, we measured protein carbonyl levels. Whereas carbonyls were unaltered under various incubation conditions in nonischemic hearts (results not shown), in IR hearts, protein carbonyl levels increased in proportion to the percentage of gassed CO_2 (Fig. 3A) and were more than 50% higher in 10% CO_2

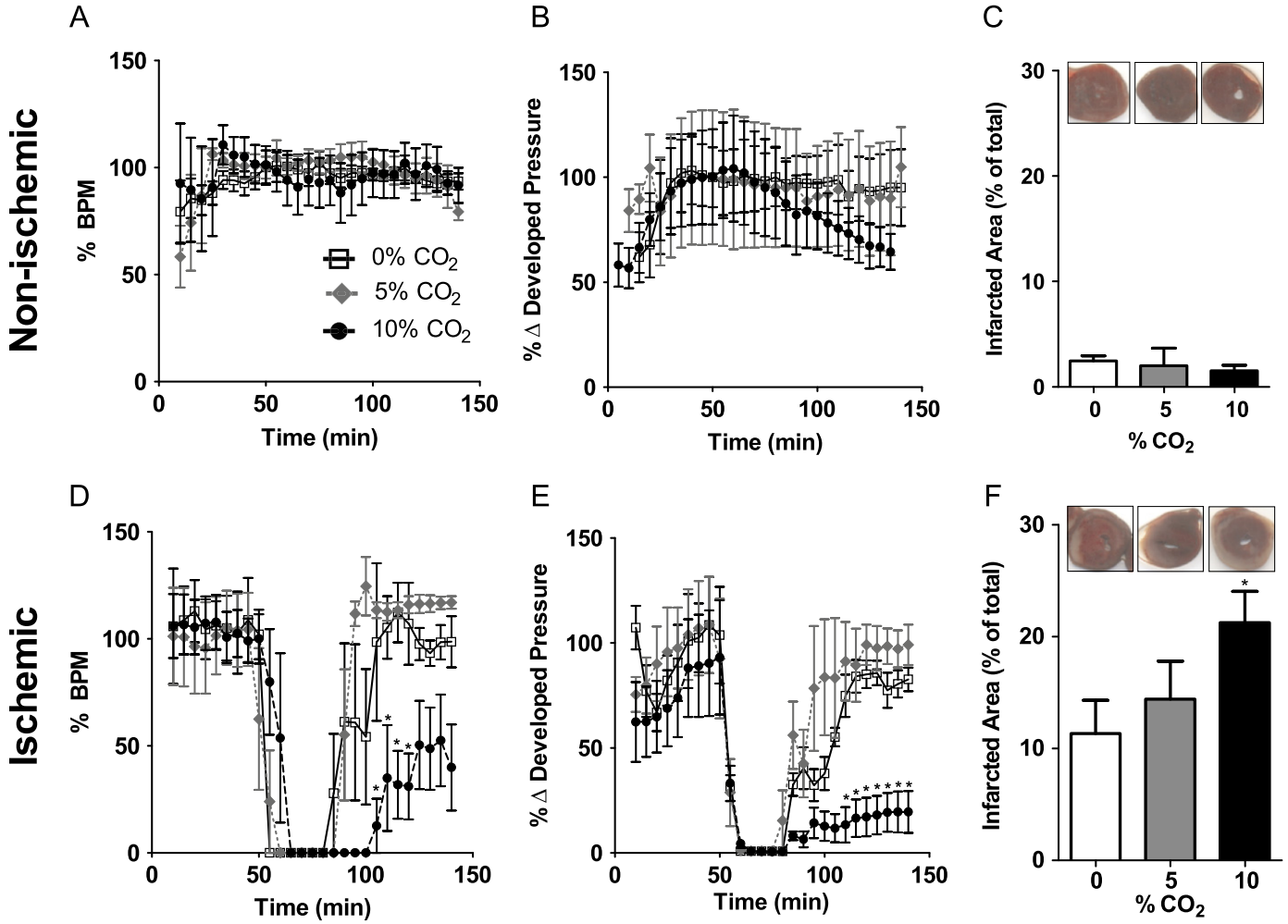

Fig. 2. Perfused rat hearts present increased functional loss when subjected to IR in the presence of 10% CO_2. (A and D) Beats per minute (BPM), (B and E) left-ventricular developed pressure, and (C and F) infarct areas were measured as described under Materials and methods for nonischemic (A–C) or IR (D–F) hearts perfused with 0, 5, or 10% CO_2. *$p < 0.05$ relative to IR with 0% CO_2.

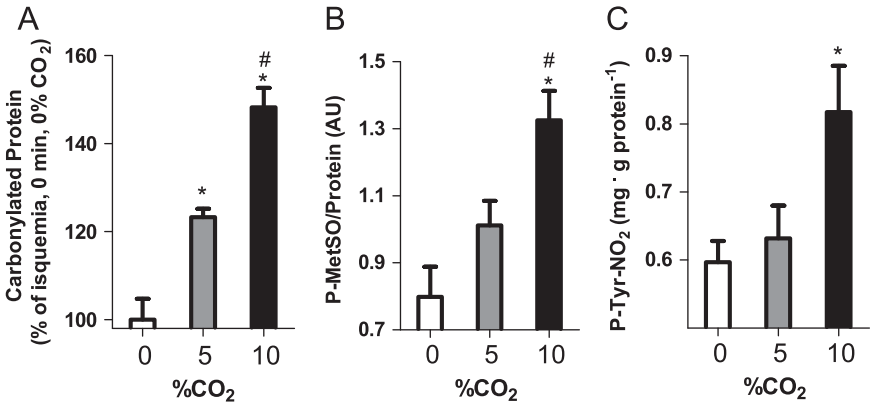

Fig. 3. Increases in CO_2 are accompanied by enhanced oxidative damage in IR hearts. The amounts of (A) carbonylated proteins, (B) methionine sulfoxide and (C) nitrotyrosine were quantified as described under Materials and methods after IR conducted under the conditions of Fig. 2. $^{*}p < 0.05$ relative to 0% CO_2; $^{\#}p < 0.05$ relative to 5% CO_2.

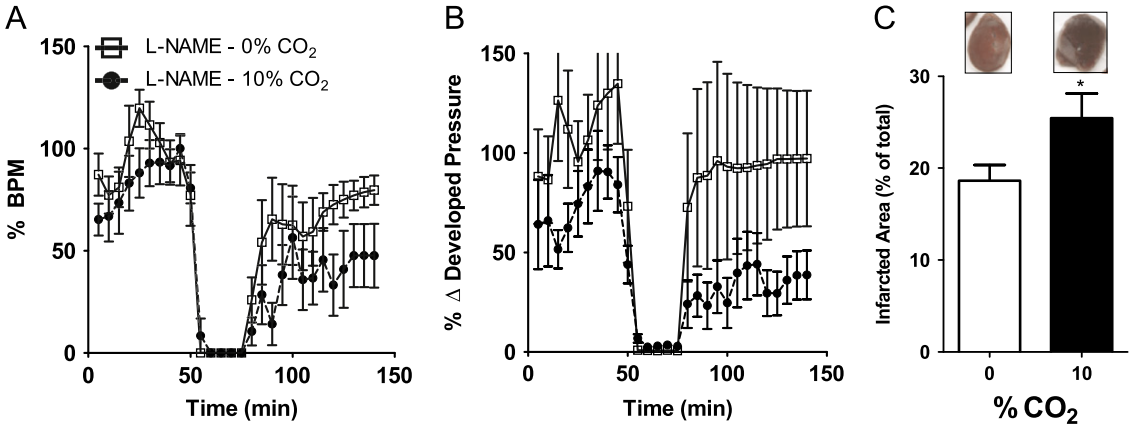

Fig. 4. L-NAME does not inhibit functional loss promoted by CO_2 in IR hearts. (A) Beats per minute (BPM), (B) left-ventricular developed pressure and (C) infarct areas were measured as for Fig. 2, with the addition of 200 μM L-NAME to the perfusion medium. $^{*}p < 0.05$ relative to 0% CO_2.

relative to the absence of this gas. Similar increases in methionine sulfoxide (Fig. 3B) and nitrotyrosine (Fig. 3C) residue levels were also observed in 10% CO_2 tissues. These protein modifications were undetectable in nonischemic heart samples perfused with any concentration of CO_2. Again, our results suggest that, although CO_2/HCO_3^- does not overtly affect hearts under physiological conditions, it is a determinant in functional and oxidative damage after IR.

The detection of increased nitrotyrosine radicals in hearts perfused with CO_2 indicates the participation of nitric oxide-derived species in cardiac damage enhanced by CO_2. Indeed, peroxynitrite in the presence of CO_2 is very efficient at promoting tyrosine nitration due to the production of nitrogen dioxide and the carbonate radical anion (reviewed in [23]). To investigate a potential role for nitric oxide-derived oxidants in this process, we measured the effects of L-NAME, an inhibitor of nitric oxide synthases, on CO_2-enhanced cardiac damage after IR (Fig. 4). We found that cardiac damage increases promoted by CO_2 persisted in the presence of L-NAME. Whereas this result suggests nitric oxide synthases are not involved in the effects of CO_2, a role for nitric oxide cannot be excluded because it can be produced through nitrite reduction during ischemia [36,44].

We next evaluated the effect of CO_2/HCO_3^- on protein carbonyl formation in *C. elegans* during anoxia–starvation as a model for worm IR. Behavior and cell morphology were also assessed in the surviving worms. We found that CO_2 had little apparent effect in the absence of AS (results not shown), whereas survival after AS was not altered by 0 or 10% CO_2 either (Fig. 5A). Protein carbonyls under AS conditions tended, nonsignificantly, to increase in 10% CO_2 (Fig. 5B). Interestingly, however, surviving animals exhibited subtle but significant differences in behavior, manifested as an increased defective response to light body wall touch as a function of CO_2 during hypoxia (Fig. 5C). The behavioral response to body wall touch is mediated by six mechanosensory neurons whose processes run just under the hypodermis of the animal. To investigate if the decrease in function in these animals was accompanied by damage to these neurons, an integrated transgene was used to label the touch cells with green fluorescent protein (GFP), and two of these neurons (PLML and PLMR) were examined in detail, as described (Materials and methods). Neuronal abnormalities that were scored included the appearance of GFP inclusions in the processes, tortuous processes, and breaks, all of which have been shown to accumulate as a result of hypoxia [9]. The incidence of such abnormalities was significantly increased by AS in 10% CO_2 compared to 0% CO_2 (Fig. 6) demonstrating that, in a whole organism model, higher CO_2/HCO_3^- promoted more significant tissue and functional damage after AS.

Discussion

Considering its role as the main biological buffer, it is surprising so little recent attention has been given to the biological activity of CO_2/HCO_3^- [14,23]. In particular, metabolic and redox effects of this buffer are expected. In this work, we evaluated the results of various tensions of CO_2, incurring at different CO_2/HCO_3^- levels.

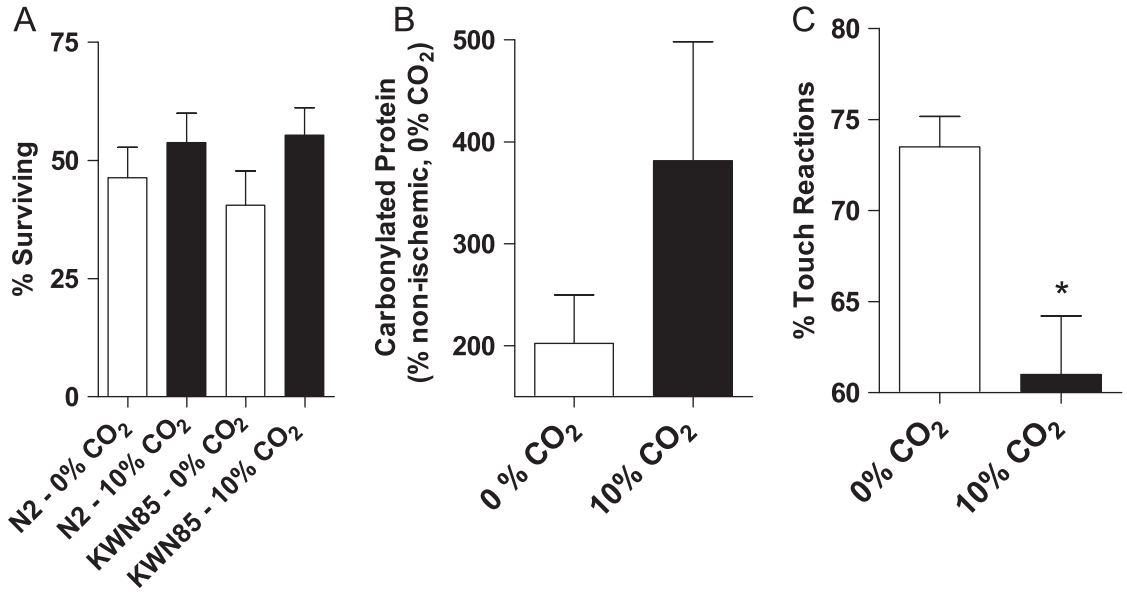

Fig. 5. 10% CO_2 decreases touch responses in *C. elegans* after IR, without affecting survival. (A) The percentage of worms that exhibit 24-h post-AS survival in the presence or absence of CO_2 was measured as described under Materials and methods. The N2 strain is the canonical wild-type genetic background, and KWN85 contains an integrated transgene that labels mechanosensory neurons with green fluorescent protein. (B) Proteins were extracted from living *C. elegans* after AS in the presence or absence of CO_2, and protein carbonyls were detected using an OxyBlot and (C) The response to touch stimuli of living *C. elegans* after AS in the presence or absence of CO_2 was measured as described under Materials and methods. $^*p < 0.01$ relative to 0% CO_2.

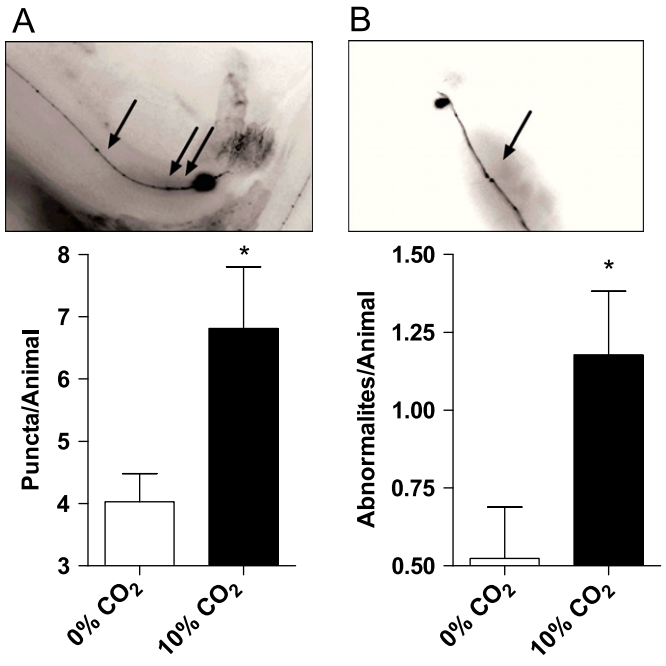

Fig. 6. 10% CO_2 increases touch neuron modifications. (A) The accumulation of GFP aggregates in the touch neuron (PLML and PLMR) processes or (B) abnormalities such as tortuous processes and breaks were monitored in surviving anesthetized *C. elegans* after IR in the presence or absence of CO_2, as described under Materials and methods. $^*p < 0.05$ relative to 0% CO_2.

Using cardiac cells, perfused rat hearts, and *C. elegans*, we found that increased CO_2/HCO_3^- heightened the injury associated with IR (Figs. 1–3) [18]. Previous studies have determined that increased levels of CO_2 result in increased heart beat rates [33], but no change in pumping function [37]. However, these changes were completely reversed by normalizing pH, indicating that they are related to pH and not to other possible biological activities of CO_2/HCO_3^-. These data, in fact, correlate well with our finding that changes in CO_2/HCO_3^- in the presence of clamped perfusion pH do not alter the basal function of perfused rat hearts (Fig. 2). On the other hand, Lavani et al. [20] found that reperfusion in the presence of high CO_2 tension resulted in protection against cardiac damage. This result differs from ours, in that we found higher cardiac damage in the presence of high CO_2 tension. Because Lavani et al. [20] did not correct for pH changes, and acidic pH is strongly protective in cardiac ischemia [19,31], it seems reasonable to propose that their effects also are attributable to pH changes promoted by altered CO_2 tension. Our work separated the pH effect of CO_2 from other biological effects by clamping pH with high concentrations of other buffers. Although we could not ascertain that this extracellular pH clamping maintained intracellular pH in perfused hearts and *C. elegans*, measured intracellular pH was identical in cells incubated in the presence and absence of CO_2/HCO_3^- (Fig. 1A), indicating that changes in pH are not necessary for the detrimental effects of CO_2.

Under these conditions, it was possible to focus on the redox effects of CO_2/HCO_3^- under basal conditions and IR. The presence of CO_2 in solution allows for the generation of the highly reactive carbonate radical from the reaction of CO_2 with peroxynitrite. CO_2 also reacts with H_2O_2, producing peroxymonocarbonate, which is a better two-electron oxidant than H_2O_2 and decomposes to the carbonate radical in the presence of biologically ubiquitous metal ions [25,29]. The carbonate radical does not produce any known stable target adducts and is therefore difficult to detect in vivo and even in vitro [23]. Peroxymonocarbonate and other oxidants may also be derived from bicarbonate. Thus, we investigated if changing CO_2/HCO_3^- altered markers of tissue redox state.

Levels of protein carbonyls, the only modification detected in the absence of IR, were not altered by CO_2/HCO_3^- under nonischemic conditions in any of the models studied. This result is not unexpected, because bicarbonate-derived oxidants are produced secondarily to reactions promoted by other reactive oxygen and nitrogen species, which are much more abundant after IR. Indeed, we found that in both cardiac cells and perfused hearts (Figs. 1 and 3), levels of oxidized proteins after IR increase markedly with the presence and increasing levels of CO_2/HCO_3^-. In fact, a linear correlation was detected between carbonylated protein ($r^2 = 0.995$, $p = 0.01$) and methionine sulfoxide ($r^2 = 0.9881$, $p = 0.06$) and CO_2 levels. Changes in protein modifications were not significantly increased in *C. elegans*, although they tended to be higher; it should be pointed out that AS

in *C. elegans* requires 20 h after reoxygenation to produce notable functional effects, and the long reperfusion time may result in the removal of many modified proteins. Despite the lack of strong evidence for changes in redox state in the *C. elegans* system, CO_2/HCO_3^- affected the functional recovery of the worms after AS (Figs. 5 and 6), once again demonstrating the importance of bicarbonate in ischemic damage.

Overall, our results show that over a wide range of experimental models (cells, organs, and whole organisms), the presence of CO_2/HCO_3^- promotes a strong decrease in function after IR, in a manner correlated with tissue oxidative damage. This demonstrates that CO_2/HCO_3^- levels are a determinant of the outcome of pathologically relevant conditions of oxidative imbalance and may explain the protective effect of modulating carbonic anhydrases [1,28]. Although CO_2/HCO_3^- are unavoidable in biological systems, our data provide a gain in the understanding of the mechanisms involved in tissue damage after ischemic insults, which we hope will be important for future development of therapeutic interventions. Furthermore, our results provide evidence, albeit indirect, for the participation of bicarbonate radicals in pathologically relevant biological processes and indicate that more attention should be focused on the redox biology of the CO_2/HCO_3^- buffer.

Acknowledgments

This work was supported by the Fundação de Amparo à Pesquisa do Estado de São Paulo (FAPESP), the Instituto Nacional de Ciência e Tecnologia de Processos Redox em Biomedicina, the Núcleo de Apoio à Pesquisa Redoxoma, USPHS NS064945 (K.N.), and USPHS GM087483 (P.S.B. and K.N.). B.B.Q. is a doctoral student supported by a FAPESP grant and an American Society for Biochemistry and Molecular Biology PROLAB award. We gratefully acknowledge Camille Caldeira da Silva, Edson Alves Gomes, and Doris Araújo for their technical support and Silvania Neves and the staff of the animal facilities for excellent animal care.

References

[1] Ahmad, S. Acetazolamide and enalapril combination offers complete protection from nitric oxide-deficient stroke in stroke-prone spontaneously hypertensive rats. *Pharmacol. Res* **41:**649–656; 2000.
[2] Arai, H.; Berlett, B. S.; Chock, P. B.; Stadtman, E. R. Effect of bicarbonate on iron-mediated oxidation of low-density lipoprotein. *Proc. Natl. Acad. Sci. USA* **102:**10472–10477; 2005.
[3] Bonini, M. G.; Miyamoto, S.; Di Mascio, P.; Augusto, O. Production of the carbonate radical anion during xanthine oxidase turnover in the presence of bicarbonate. *J. Biol. Chem.* **279:**51836–51843; 2004.
[4] Brenner, S. The genetics of *Caenorhabditis elegans*. *Genetics* **77:**71–94; 1974.
[5] Budas, G. R.; Disatnik, M. H.; Chen, C. H.; Mochly-Rosen, D. Activation of aldehyde dehydrogenase 2 (ALDH2) confers cardioprotection in protein kinase C epsilon (PKCvarepsilon) knockout mice. *J. Mol. Cell. Cardiol.* **48:**757–764; 2010.
[6] Cardoso, A. R.; Chausse, B.; da Cunha, F. M.; Luévano-Martínez, L. A.; Marazzi, T. B. M.; Pessoa, P. S.; Queliconi, B. B.; Kowaltowski, A. J. Mitochondrial compartmentalization of redox processes. *Free Radic. Biol. Med.* **52:**2201–2208; 2012.
[7] Claycomb, W. C.; Lanson Jr N. A.; Stallworth, B. S.; Egeland, D. B.; Delcarpio, J. B.; Bahinski, A.; Izzo Jr. N. J. HL-1 cells: a cardiac muscle cell line that contracts and retains phenotypic characteristics of the adult cardiomyocyte. *Proc. Natl. Acad. Sci. USA* **95:**2979–2984; 1998.
[8] da Cunha, F. M.; Demasi, M.; Kowaltowski, A. J. Aging and calorie restriction modulate yeast redox state, oxidized protein removal, and the ubiquitin–proteasome system. *Free Radic. Biol. Med.* **51:**664–670; 2011.
[9] Dasgupta, N.; Patel, A. M.; Scott, B. A.; Crowder, C. M. Hypoxic preconditioning requires the apoptosis protein CED-4 in C. elegans. *Curr. Biol.* **17:**1954–1959; 2007.
[10] Ezraty, B.; Chabalier, M.; Ducret, A.; Maisoneuve, E.; Dukan, S. CO_2 exacerbates oxygen toxicity. *EMBO Rep.* **12:**321–326; 2011.
[11] Facundo, H. T.; de Paula, J. G.; Kowaltowski, A. J.; Mitochondrial ATP-sensitive, K channels prevent oxidative stress, permeability transition and cell death. *J. Bioenerg. Biomembr.* **37:**75–82; 2005.
[12] Facundo, H. T.; Carreira, R. S.; de Paula, J. G.; Santos, C. C.; Ferranti, R.; Laurindo, F. R.; Kowaltowski, A. J. Ischemic preconditioning requires increases in reactive oxygen release independent of mitochondrial K^+ channel activity. *Free Radic. Biol. Med.* **40:**469–479; 2006.
[13] Fishbein, M. C.; Meerbaum, S.; Rit, J.; Lando, U.; Kanmatsuse, K.; Mercier, J. C.; Corday, E.; Ganz, W. Early phase acute myocardial infarct size quantification: validation of the triphenyl tetrazolium chloride tissue enzyme staining technique. *Am. Heart J.* **101:**593–600; 1981.
[14] Guais, A.; Brand, G.; Jacquot, L.; Karrer, M.; Dukan, S.; Grévillot, G.; Molina, T. J.; Bonte, J.; Regnier, M.; Schwartz, L. Toxicity of carbon dioxide: a review. *Chem. Res. Toxicol.* **24:**2061–2070; 2011.
[15] Hodgson, E. K.; Fridovich, I. The mechanism of the activity-dependent luminescence of xanthine oxidase. *Arch. Biochem. Biophys.* **172:**202–205; 1976.
[16] Johnson, D.; Nehrke, K. Mitochondrial fragmentation leads to intracellular acidification in Caenorhabditis elegans and mammalian cells. *Mol. Biol. Cell* **21:**2191–2201; 2010.
[17] Karsten, U. Fluorometric estimation of dead cells in cell suspensions. *Experientia* **36:**263–264; 1980.
[18] Khandoudi, N.; Bernard, M.; Cozzone, P.; Feuvray, D. Mechanisms of intracellular pH regulation during postischemic reperfusion of diabetic rat hearts. *Diabetes* **44:**196–202; 1995.
[19] Kitakaze, M.; Weisfeldt, M. L.; Marban, E. Acidosis during early reperfusion prevents myocardial stunning in perfused ferret hearts. *J. Clin. Invest.* **82:**920–927; 1988.
[20] Lavani, R.; Chang, W. T.; Anderson, T.; Shao, Z. H.; Wojcik, K. R.; Li, C. Q.; Pietrowski, R.; Beiser, D. G.; Idris, A. H.; Hamann, K. J.; Becker, L. B.; Vanden Hoek, T. L. Altering CO_2 during reperfusion of ischemic cardiomyocytes modifies mitochondrial oxidant injury. *Crit. Care Med.* **35:**1709–1716; 2007.
[21] Liochev, S. I.; Fridovich, I. CO_2, not HCO_3^- facilitates oxidations by Cu,Zn superoxide dismutase plus H_2O_2. *Proc. Natl. Acad. Sci. USA* **101:**743–744; 2004.
[22] Martin, A.; Zulueta, J.; Hassoun, P.; Blumberg, J. B.; Meydani, M. Effect of vitamin E on hydrogen peroxide production by human vascular endothelial cells after hypoxia/reoxygenation. *Free Radic. Biol. Med.* **20:**99–105; 1996.
[23] Medinas, D. B.; Cerchiaro, G.; Trindade, D. F.; Augusto, O. The carbonate radical and related oxidants derived from bicarbonate buffer. *IUBMB Life* **59:**255–262; 2007.
[24] Medinas, D. B.; Toledo Jr J. C.; Cerchiaro, G.; do-Amaral, A. T.; de-Rezende, L.; Malvezzi, A.; Augusto, O. Peroxymonocarbonate and carbonate radical displace the hydroxyl-like oxidant in the Sod1 peroxidase activity under physiological conditions. *Chem. Res. Toxicol.* **22:**639–648; 2009.
[25] Medinas, D. B.; Augusto, O. Mechanism of the peroxidase activity of superoxide dismutase. *Free Radic. Biol. Med.* **49:**682; 2010.
[26] Nakamura, A.; Goto, S. Analysis of protein carbonyls with 2,4-dinitrophenyl hydrazine and its antibodies by immunoblot in two-dimensional gel electrophoresis. *J. Biochem* **119:**768–774; 1996.
[27] Radi, R. Nitric oxide, oxidants, and protein tyrosine nitration. *Proc. Natl. Acad. Sci. USA* **101:**4003–4008; 2004.
[28] Räisänen, S. R.; Lehenkari, P.; Tasanen, M.; Rahkila, P.; Härkönen, P. L.; Väänänen, H. K. Carbonic anhydrase III protects cells from hydrogen peroxide-induced apoptosis. *FASEB J.* **13:**513–522; 1999.
[29] Ramirez, D. C.; Mejiba, S. E.; Mason, R. P. Copper-catalyzed protein oxidation and its modulation by carbon dioxide: enhancement of protein radicals in cells. *J. Biol. Chem.* **280:**27402–27411; 2005.
[30] Rink, T. J.; Tsien, R. Y.; Pozzan, T. Cytoplasmic pH and free Mg^{2+} in lymphocytes. *J. Cell Biol.* **95:**189–196; 1982.
[31] Schäfer, C.; Ladilov, Y. V.; Siegmund, B.; Piper, H. M. Importance of bicarbonate transport for protection of cardiomyocytes against reoxygenation injury. *Am. J. Physiol. Heart Circ. Physiol* **278:**H1457–1463; 2000.
[32] Scott, B. A.; Avidan, M. S.; Crowder, C. M. Regulation of hypoxic death in C. elegans by the insulin/IGF receptor homolog DAF-2. *Science* **296:**2388–2391; 2002.
[33] Stinson, J. M.; Mattsson, J. L. Tolerance of rhesus monkeys to graded increase in environmental CO_2: serial changes in heart rate and cardiac rhythm. *Aerosp. Med* **41:**415–418; 1970.
[34] Surmeli, N. B.; Litterman, N. K.; Miller, A. F.; Groves, J. T. Peroxynitrite mediates active site tyrosine nitration in manganese superoxide dismutase: evidence of a role for the carbonate radical anion. *J. Am. Chem. Soc.* **132:**17174–17185; 2010.
[35] Vanden Hoek, T. L.; Shao, Z.; Li, C.; Zak, R.; Schumacker, P. T.; Becker, L. B. Reperfusion injury on cardiac myocytes after simulated ischemia. *Am. J. Physiol.* **270:**H1334–1341; 1996.
[36] Webb, A.; Bond, R.; McLean, P.; Uppal, R.; Benjamin, N.; Ahluwalia, A. Reduction of nitrite to nitric oxide during ischemia protects against myocardial ischemia–reperfusion damage. *Proc. Natl. Acad. Sci. USA* **101:**13683–13688; 2004.
[37] Wexels, J. C.; Mjøs, O. D. Effects of carbon dioxide and pH on myocardial function in dogs with acute left ventricular failure. *Crit. Care Med* **15:**1116–1120; 1987.
[38] White, S. M.; Constantin, P. E.; Claycomb, W. C. Cardiac physiology at the cellular level: use of cultured HL-1 cardiomyocytes for studies of cardiac muscle cell structure and function. *Am. J. Physiol. Heart Circ. Physiol* **286:**H823–829; 2004.
[39] Winterbourn, C. C. Reconciling the chemistry and biology of reactive oxygen species. *Nat. Chem. Biol.* **4:**278–286; 2008.
[40] Wojtovich, A. P.; Sherman, T. A.; Nadtochiy, S. M.; Urciuoli, W. R.; Brookes, P. S.; Nehrke, K. SLO-2 is cytoprotective and contributes to mitochondrial potassium transport. *PLoS One* 6; 2011*e28287* 6; 2011.

[41] Wojtovich, A. P.; DiStefano, P.; Sherman, T.; Brookes, P. S.; Nehrke, K. Mitochondrial ATP-sensitive potassium channel activity and hypoxic preconditioning are independent of an inwardly rectifying potassium channel subunit in *Caenorhabditis elegans*. *FEBS Lett* **586:**428–434; 2012.

[42] Zhang, H.; Andrekopoulos, C.; Joseph, J.; Chandran, K.; Karoui, H.; Crow, J. P.; Kalyanaraman, B. Bicarbonate-dependent peroxidase activity of human Cu,Zn-superoxide dismutase induces covalent aggregation of protein: intermediacy of tryptophan-derived oxidation products. *J. Biol. Chem.* **278:**24078–24089; 2003.

[43] Zhou, H.; Singh, H.; Parsons, Z. D.; Lewis, S. M.; Bhattacharya, S.; Seiner, D. R.; LaButti, J. N.; Reilly, T. J.; Tanner, J. J.; Gates, K. S. The biological buffer bicarbonate/CO_2 potentiates H_2O_2-mediated inactivation of protein tyrosine phosphatases. *J. Am. Chem. Soc.* **133:**15803–15805; 2011.

[44] Zweier, J. L.; Wang, P.; Samouilov, A.; Kuppusamy, P. Enzyme-independent formation of nitric oxide in biological tissues. *Nat. Med* **1:**804–809; 1995.